Proceedings of the 11th World Congress on Mechanical, Chemical, and Material Engineering (MCM'25)

Paris, France - August, 2025 Paper No. ICMIE 167 DOI: 10.11159/icmie25.167

# Rheological Calibration and CFD Simulation of Grease Behaviour Using the Herschel-Bulkley Model

Michele Benetti<sup>1</sup>, Lorenzo Maccioni<sup>1</sup>, Kay Juckelandt<sup>2</sup>, Michael Plogmann<sup>2</sup>, Franco Concli<sup>1</sup>

<sup>1</sup>Free University of Bozen-Bolzano, Faculty of Engineering via Bruno Buozzi, 1, 39100, Bolzano, Italy

<sup>2</sup>Schaeffler Technologies AG & Co. KG, Industriestrasse 1–3, 91074 Herzogenaurach, Germany michele.benetti@student.unibz.it; lorenzo.maccioni@unibz.it; kay.juckelandt@schaeffler.com; michael.plogmann@schaeffler.com; franco.concli@unibz.it.

**Abstract** - This paper represents a first step within a broader research project aimed at developing Computational Fluid Dynamics (CFD) models capable of reliably predicting the flow behavior of lubricating greases in mechanical systems, with the ultimate objective of estimating load-independent power losses and analyzing grease distribution. In this initial phase, the authors focus on the rheological characterization of a bearing grease through experimental measurements performed on a cone-on-plate rheometer at two temperatures: 25°C and 80°C. The Herschel-Bulkley (HB) model was selected due to its widespread adoption in modeling non-Newtonian fluids like grease. A curve-fitting procedure was employed to calibrate the HB parameters (yield stress, consistency index, and flow index) using various regression strategies: Mean Squared Error, Percentage Error, Absolute Error, and Logarithmic Error. Among them, the logarithmic error minimization approach provided the best agreement with the experimental data. The sensitivity of model accuracy to the chosen fitting criterion is discussed. The optimized HB parameters were then used to simulate the experimental setup in the open-source environment OpenFOAM®, modeling a rotational sector of the rheometer by exploiting its cyclic symmetry. A structured hexahedral mesh was generated, and a mesh sensitivity analysis was carried out to ensure solution robustness. Although the physical system is steady and single-phase, a transient two-phase solver was adopted to align with the long-term goal of simulating grease-air interactions in real-world applications such as rolling-element bearings. The simulation results confirmed the theoretical assumption of nearly uniform shear rate across the cone-plate gap and demonstrated excellent agreement between the predicted and measured torques. Additionally, a clear influence of temperature on HB parameters was observed, emphasizing the need for temperature-specific calibration.

Keywords: Grease; Lubrication; Non-Newtonian; Shear Stress; Shear Rate; Viscosimeter; CFD; OpenFOAM®.

#### 1. Introduction

In recent years, Computational Fluid Dynamics (CFD) has become an increasingly adopted tool for modeling the behavior of lubricants within mechanical components [1,2]. However, while over 80% of bearings in industrial applications are grease-lubricated [3], the use of CFD to study grease lubrication remains limited [1,2]. The majority of existing studies have primarily focused on oil lubrication (e.g., [4-14]), whereas fewer efforts have targeted grease-lubricated systems (e.g., [15-23]).

One of the major challenges in modeling grease flow is its proper rheological characterization. Indeed, as demonstrated by Forster and Kolfenbach [24], greases show viscoelastic properties. Moreover, grease exhibits a complex non-Newtonian behavior, where the relationship between shear stress and shear rate is influenced by several factors, including temperature, aging, and mechanical pre-shearing. While effective lubrication can be and is ensured in practice through experimental procedures, operational experience, and empirical design rules, the accurate prediction of grease behavior within a bearing via computational models remains challenging. The use of CFD to simulate grease flow is limited by the complexity of its rheological response, making purely numerical predictions of hydrodynamic losses or grease distribution unreliable without experimental validation. As a result, physical experiments — although expensive and time-consuming — are often required both to assess product reliability in service conditions and to support the development and refinement of numerical models.

Traditionally, the solid-like behavior or resistance to flow of a grease is assessed through consistency or penetration tests using cone penetrometers (ISO 2137, ASTM D217), which yield an NLGI consistency number. An alternative approach

involves the direct measurement of the yield stress using rheometers, either through computerized evaluation methods (e.g., CEY by Gow [25]) or stress crossover techniques (e.g., Couronné et al. [26]). These methods, however, are typically performed at room temperature and do not account for in-service conditions.

Several rheological models have been proposed to describe their flow behavior across a range of shear rates, including the Power Law [27], Rhee-Eyring [28], Bingham [29,30], and Herschel–Bulkley (HB) [31] models. Among these, the HB model is particularly suited for grease simulation in mechanical components [32]. It combines a yield stress threshold ( $\tau_0$ ) with a power-law term that captures shear-thinning behavior at moderate to high shear rates. The HB equation is typically expressed as:

$$\tau = \tau_0 + \mathbf{K} \cdot \dot{\mathbf{y}}^n \tag{1}$$

where:

- $\tau = \text{shear stress } [Pa]$
- $\tau_0$  = yield stress [Pa]
- $K = consistency index [Pa \cdot s^n]$
- n = flow index [dimensionless]
- $\dot{\gamma}$  = shear rate [s<sup>-1</sup>]

These parameters can be calibrated by fitting experimental data obtained under controlled conditions.

In this work, an experimental procedure for calibrating the HB model parameters is followed up, using a cone-on-plate rheometer (Anton Paar CP25-1/TG). The specific geometry of the device allows for the accurate transformation of measured torque and rotational speed into shear stress and shear rate using well-defined calibration constants [33]. This method can be performed at varying temperatures, speeds, and grease conditions (including aged or pre-sheared samples), making it suitable for replicating service-like environments.

The overall goal of this study is to establish a validated methodology for the rheological characterization of grease to support its implementation in CFD simulations. Section 2.1 presents the overview of the proposed methodology, Section 2.2 details the experimental setup and data processing approach, and Section 2.3 describes the CFD model developed based on the HB parameters. Results and discussion are provided in Section 3, followed by the main conclusions in Section 4.

#### 2. Materials and Methods

## 2.1. General methodology

To verify that the HB model follows the grease's rheological behaviour, both CFD simulations and experimental results must exhibit the same correlation between the characteristic parameters—namely, the resistant torque and angular velocity—measured using a rheometer. Since the shear rate is defined as the ratio between angular velocity and fluid thickness, it can be assumed constant in a cone-on-plate rheometer.

The CFD simulation based on the HB model requires the three parameters introduced earlier:  $\tau_0$ , K, and n. These parameters must be determined by fitting the experimental data. This fitting process was carried out in Matlab: given the experimental values, the equation that minimise the following errors has been defined.

Various numerical regression methods were tested to determine which provided the best fit between the experimental data. The different numerical regression methods rely on minimizing the following errors.

$$MSE = \sum ((\tau_0 + K \cdot \dot{\gamma}^n) - \tau)^2$$
 (2)

where MSE = Mean Squared Error. It minimizes the sum of squared deviations between the model predictions and experimental data

$$PE = \sum \left| \frac{\left( \tau_0 + K \cdot \dot{y}^n \right) - \tau}{\tau} \right| \tag{3}$$

where PE = Percentage Error. It minimizes the relative error between the model and experimental data.

$$LOG = \sum \left( log \left( \tau_0 + K \cdot \dot{\gamma}^n \right) - log \left( \tau \right) \right)^2 \tag{4}$$

where LOG = Logarithmic Error. It minimizes the logarithmic difference between the model and experimental data.

$$ABS = \sum |(\tau_0 + K \cdot \dot{\gamma}^n) - \tau| \tag{5}$$

where ABS = Absolute Error. It minimizes the sum of absolute deviations between the model and experimental data. Once the numerical regression models are defined, the one that best fits the experimental data is identified. The corresponding parameters,  $\tau_0$ , K, and n, are then implemented in the CFD software. The results of the CFD simulation are subsequently compared with the experimental measurements.

## 2.2. Experimental

A cone-on-plate rheometer configuration has been considered. The moving part is set in motion on the vertical axis. The measurements have been carried out using a specific grease for rolling element bearings. Each series of measurements has been conducted following the DIN 51810-1 to keep 16 points at different shear rate ranging from 0.1 [1/s] to 10000 [1/s]. The time interval between every measuring point was 10 seconds and, for each rotational speed, the resistant torque has been measured. Exploiting the specific constant of the rheometer (CSD, and CSR), according to the ISO 3219, it has been possible to obtain the relation between the shear rate and the shear stress. These series of measurements have been repeated twice (Exp.1 and Exp.2 in Fig. 3) for each investigated temperature of 25°C and 80°C. The acquisition frequency carried out in the experiments is 0.1 Hz. The plots of the values of the resistant torque vs. the angular velocity are shown in Fig. 3. In the present paper, the values of torque and shear rate has been made dimensionless.

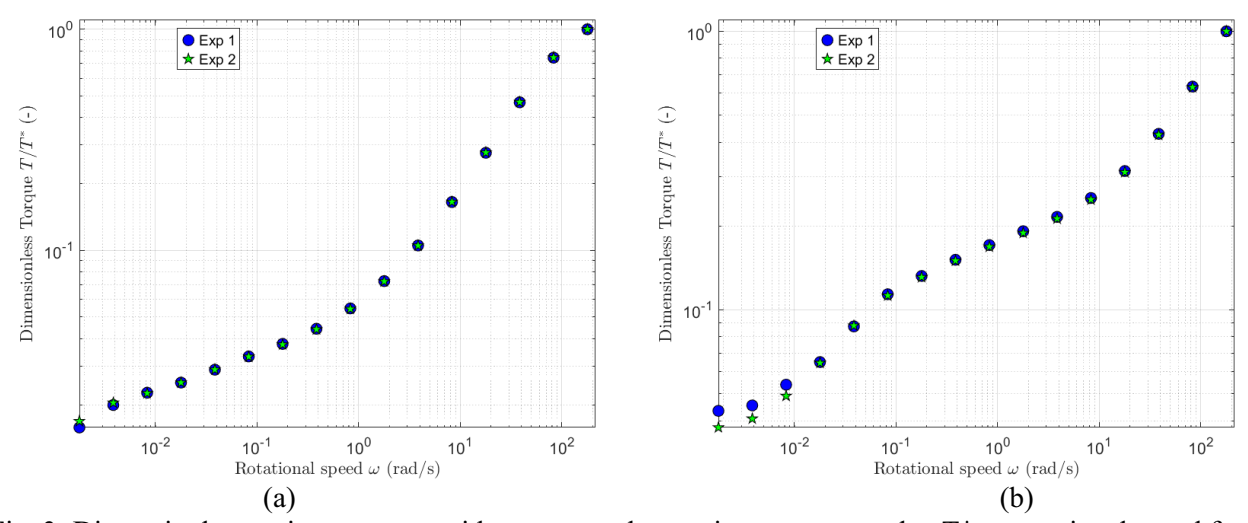


Fig. 3: Dimensionless resistant torque with respect to the maximum torque value T\* vs rotational speed for the first experiment at 25°C (a) and 80°C (b).

## 2.3. Numerical approach

CFD simulations were performed using OpenFOAM®, an open-source software based on the finite-volume method, which is widely customizable and adjustable to perform various types of physical simulations, including fluid dynamics ones. Solvers, utilities and pre/postprocessing tools can be modified and adapted, making it flexible for both research and industrial

use. Numerous studies in the literature employ this software to model the fluid dynamics of bearings, which constitutes the long-term objective of the broader research framework to which this project belongs.

## 2.4. Mesh, initial conditions and boundary conditions

The geometry of the rheometer is symmetric with respect to the vertical axis and, in this study, the gravity acts along the vertical axis. Therefore, in order to reduce the computational effort, the axial-symmetry (cyclic-symmetry) of this system has been exploited. The computational domain has been discretised using the *blockMesh* utility to obtain a parametric structured mesh i.e. composed by hexahedral cells exclusively. In addition, this approach enables a controlled mesh grading. The volume modelled with *blockMesh* represents a sector of 2 degrees out of 360. To get only hexahedral cells, the central tip of the computational domain has been approximated; this part lead to a negligible contribution of the resulting torque, then this approximation can be easily justified for the goal of the simulations. Moreover, the external part of the computational domain has been modelled with a toroidal geometry in order to take into considerations also the edge effects. In Fig. 5, the different patches and an example of the grid can be observed. The *wall*-type boundary conditions "cone" and "cylinder" represent the grease in contact with the moving part of the rheometer. The patch "inletOutlet" indicates the interface between grease and outer space. The relative pressure on this patch was set to zero. The *wall*-type boundary condition "plane" was applied to the stationary part of the rheometer. Two *cyclic*-type BCs were applied to the lateral faces to model the cyclic symmetry of the grease portion.

The velocities were assigned to the patches using appropriate BCs. The *rotatingWallVelocity* BC (with rotational axis and speed inputs defined via a dictionary) was used to impose the velocities of the moving part of the rheometer. The *rotatingWallVelocity* is a BC that provides a rotational velocity condition for a boundary consisting of a rotating solid of revolution, e.g. cylinder/cone.

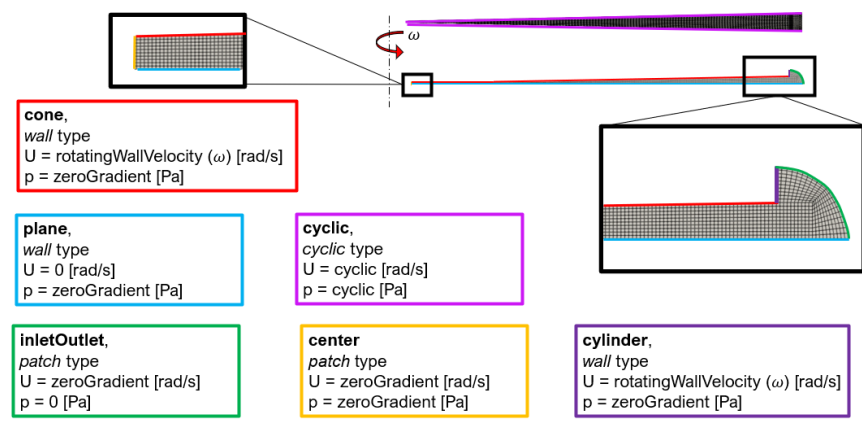


Fig. 5: computational domain and boundary conditions

The computational domain was assumed to be partially filled with grease; in the external part, air has been modelled. The initial conditions are shown in Fig. 6.

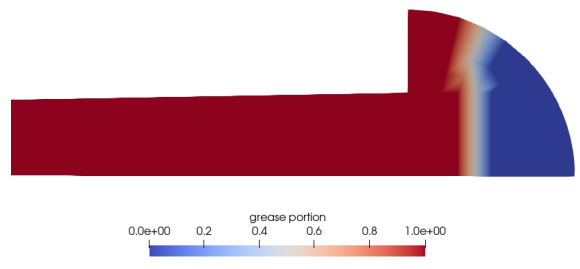


Fig. 6: distribution of grease (red) and air (blue) at time t=0 [s]; zoom of the external part

#### 2.5. Solver

A two-phase, incompressible, laminar, and transient solver was exploited in the present work. The mass and momentum equations were solved assuming the system as isothermal. Simulations have been carried out limiting the Courant number (Co) to 0.9 to ensure the stability and convergence of the numerical solution. This type of solver was chosen because the present work is a preliminary study intended to support future investigations on the behaviour of multiphase flows inside rolling bearings. In such applications, a transient two-phase solver will be required. Therefore, it has been adopted and finetuned from this early stage, even though simpler simulation models exist. An adjustabletimestep setting was used, starting from an initial  $\Delta t$  chosen to ensure a Courant number below 0.01. As the simulation progressed,  $\Delta t$  increased until reaching a Co below 0.9. The convergence of the simulation was defined based on the evaluation of the resistant torque. Specifically, the simulation was considered converged when the torque variation remained below the fourth decimal place for 50 consecutive timesteps. A preliminary mesh sensitivity study was conducted for a single value of rotational speed, to verify that the percentage error between the resulting torque was under 0.05%. Fig. 7 shows the values of the dimensionless torque for each mesh configuration used. As can be observed, the percentage error in the torque remains below 1% for the majority of the tests. This indicates that it is possible to achieve a high level of accuracy in the simulations also with relatively low numbers of cells while significantly reducing computational time. Consequently, for the simulations performed at different angular velocities, a mesh consisting of 3125 elements was selected, as it was considered a good compromise between computational effort and the accuracy of the results.

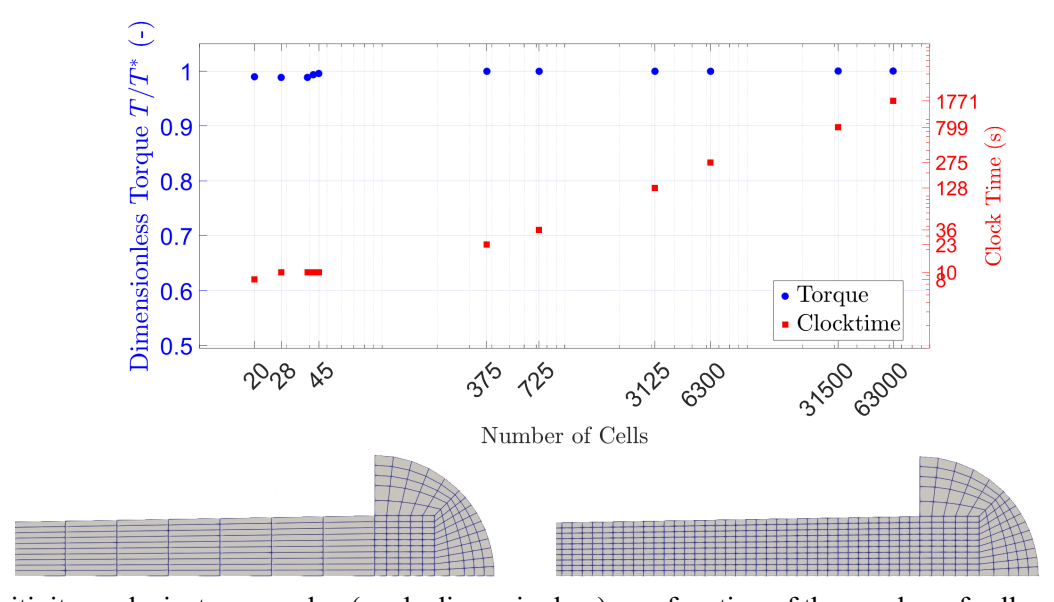


Fig. 7: mesh sensitivity analysis: torque value (made dimensionless) as a function of the number of cells and computational time for each simulation. A portion of a mesh with 725 cells (left) and one with 3125 (right) cells.

## 3. Results and discussion

## 3.1. Herschel-Bulkley Fit

In Fig. 8 the dimensionless experimental shear stress values as a function of shear rate, along with the fitted curves obtained using the different error minimization methods described in subsection 2.1 are shown. It can be noted that each fitting approach yields different sets of HB model parameters. Among them, the method based on logarithmic error minimization appears to provide the best approximation of the experimental data at both temperatures. The corresponding values of  $\tau_0$ , K, and n were therefore implemented in the CFD software to run the simulations. As mentioned before, the numerical regressions used to determine the coefficients of the HB model were based on the assumption that the CCS factor of the rheometer could be used to convert angular velocity into shear rate and torque into shear stress, according to the above-mentioned standards.

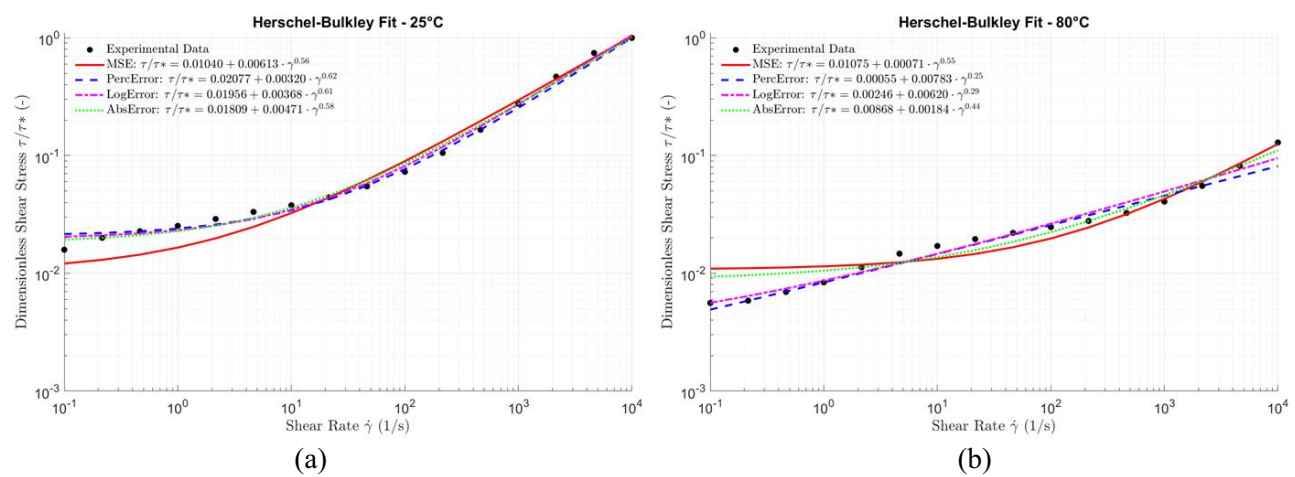


Fig. 8: comparison between different regression approaches for the HB equation on experimental data recorded at 25°C (a) and 80°C (b).

## 3.2. CFD vs Experimental Torque Comparison

In Fig. 9, a comparison is presented between the experimental/CFD/fitted results achieved in this article for the values of torque, dimensionless, as a function of the rotational speed. Results for  $25^{\circ}$ C and  $80^{\circ}$ C are presented on the left and right sides of Fig. 9, respectively. It can be observed that the CFD and fitted results are in good agreement across all values of  $\omega$  and at both temperatures. At  $25^{\circ}$ C, the CFD results closely approximate the experimental data within the tested angular velocity range (0.003841 to 178.3 rad/s). However, some discrepancies remain at the lower end of the range, where the CFD and the analytical results do not fully align with the experimental measurements. At  $80^{\circ}$ C, the agreement between CFD and experimental results is less consistent. While only minor differences are observed at intermediate  $\omega$  values, more significant deviations appear at medium-high and high angular velocities. Possible causes for the mismatch between CFD and experimental results, especially at high temperatures, may lie in the fact that the energy equation was not included in the simulations, assuming the grease as an isothermal fluid according to the standards. As a result, potential thermal gradients within the domain were not accounted for. Furthermore, it should be noted that the HB model, while widely used for grease flow characterization, might also present limitations in accurately capturing the temperature-dependent rheological behavior of grease. This could contribute to the observed discrepancies, particularly under thermal conditions where the grease's viscosity and yield stress are expected to vary significantly.

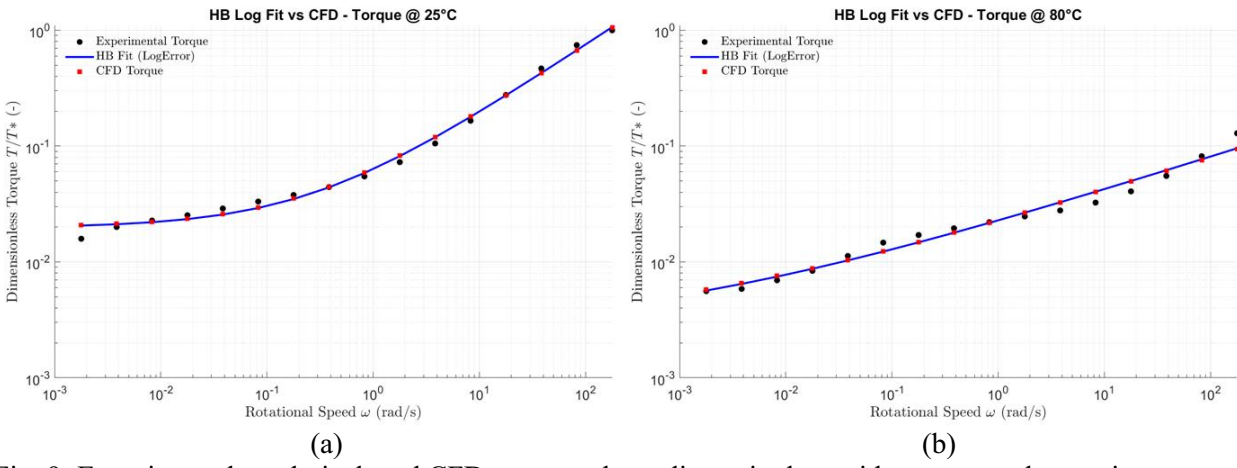


Fig. 9: Experimental, analytical, and CFD torque values, dimensionless with respect to the maximum torque value T\*, as a function of the rotational speed, at 25°C (a) and 80°C (b).

## 4. Conclusions

This work presented a methodology for the rheological characterization and CFD modelling of a lubricating grease using the HB model. Experimental tests were carried out at two temperatures (25 °C and 80 °C) using a cone-on-plate rheometer, and the HB parameters were identified through different numerical regression techniques. Among the tested methods, the logarithmic error minimization provided the best fit with the experimental data across both temperature conditions. The extracted HB parameters were then implemented in OpenFOAM® to simulate the rheometer's flow conditions. A mesh sensitivity analysis was performed, and a computationally efficient mesh configuration was selected without compromising accuracy. The use of a transient two-phase solver—selected to anticipate future simulations involving grease-air interactions in bearings—lead to a good agreement between CFD predictions and experimental data, especially at 25 °C. Some deviations were observed at higher temperatures and angular velocities, likely due to the absence of the energy equation and unaccounted thermal gradients. Overall, the methodology demonstrated in this study represents a foundation for future investigations into grease behaviour in mechanical systems.

## **Acknowledgements**

Funded by the European Union- Next Generation EU, Mission 4 Component 1 CUP I52B24000510005 and HyperCUBE Project, financed by Schaeffler Technologies AG & Co. KG, PI F. Concli.

#### References

- [1] L. Maccioni and F. Concli, "Computational fluid dynamics applied to lubricated mechanical components: Review of the approaches to simulate gears, bearings, and pumps," *Appl. Sci.*, 2020, vol. 10, no. 24, pp. 8810.
- [2] F. Sadeghi, U. Arya, S. Aamer, and A. Meinel, "A review of computational fluid dynamics approaches used to investigate lubrication of rolling element bearings," *J. Tribol.*, 2024, vol. 146, no. 10, pp. 100801.
- [3] P. M. Lugt, "Modern advancements in lubricating grease technology," Tribol. Int., 2016, vol. 97, pp. 467–477.
- [4] F. Concli, C. T. Schaefer, and C. Bohnert, "Innovative meshing strategies for bearing lubrication simulations," Lubricants, 2020, vol. 8, no. 4, Art. no. 46.
- [5] A. Gonda, D. Großberndt, B. Sauer, and H. Schwarze, "Experimental and numerical investigations of hydraulic losses in rolling bearings under practice-oriented conditions," *Tribol. Schmier.*, 2018, vol. 65, pp. 7–13.
- [6] A. Feldermann, D. Fischer, S. Neumann, and G. Jacobs, "Determination of hydraulic losses in radial cylindrical roller bearings using CFD simulations," *Tribol. Int.*, 2017, vol. 113, pp. 245–251.
- [7] J. Hu, W. Wu, M. Wu, and S. Yuan, "Numerical investigation of the air—oil two-phase flow inside an oil-jet lubricated ball bearing," *Int. J. Heat Mass Transf.*, 2014, vol. 68, pp. 85–93.
- [8] J. Liebrecht, X. Si, B. Sauer, and H. Schwarze, "Investigation of drag and churning losses on tapered roller bearings," *Stroj. Vestn. J. Mech. Eng.*, 2015, vol. 61, no. 6, pp. 399–408.
- [9] L. Maccioni, V. G. Chernoray, and F. Concli, "Fluxes in a full-flooded lubricated tapered roller bearing: Particle image velocimetry measurements and computational fluid dynamics simulations," *Tribol. Int.*, 2023, vol. 188, p. 108824.
- [10] L. Maccioni, L. Rüth, O. Koch, and F. Concli, "Load-independent power losses of fully flooded lubricated tapered roller bearings: Numerical and experimental investigation of the effect of operating temperature and housing wall distances," *Tribol. Trans.*, 2023, vol. 66, no. 6, pp. 1078–1094.
- [11] L. Maccioni, V. G. Chernoray, and F. Concli, "Investigating lubricant behavior in a partially flooded tapered roller bearing: Validation of a multiphase CFD solver for aerated oil sump via particle image velocimetry studies and high-speed camera acquisitions," *Tribol. Int.*, 2025, vol. 201, p. 110274.
- [12] S. Aamer, F. Sadeghi, T. Russell, W. Peterson, A. Meinel, and H. Grillenberger, "Lubrication, flow visualization, and multiphase CFD modeling of ball bearing cage," *Tribol. Trans.*, 2022, vol. 65, no. 6, pp. 1088–1098.
- [13] W. Peterson, T. Russell, F. Sadeghi, M. T. Berhan, L.-E. Stacke, and J. Ståhl, "A CFD investigation of lubricant flow in deep groove ball bearings," *Tribol. Int.*, 2021, vol. 154, p. 106735.
- [14] U. Arya, W. Peterson, F. Sadeghi, A. Meinel, and H. Grillenberger, "Investigation of oil flow in a ball bearing using bubble image velocimetry and CFD modeling," *Tribol. Int.*, 2023, vol. 177, p. 107968.

- [15] T. Noda, K. Shibasaki, S. Miyata, and M. Taniguchi, "X-ray CT imaging of grease behavior in ball bearing and numerical validation of multi-phase flows simulation," *Tribol. Online*, 2020, vol. 15, no. 1, pp. 36–44.
- [16] B. Wang, Z. Wang, C. Sun, and Y. Wu, "Numerical investigation of the heat-fluid characteristic inside high-speed angular contact ball bearing lubricated with grease," *Int. J. Eng.*, 2021, vol. 34, no. 5, pp. 1313–1320.
- [17] Q. Wang, "Research on the lubricating grease distribution patterns of the beam pumping unit in the oil and petrochemical industry," in 2023 3rd Int. Conf. Electrical Eng. Control Sci. (IC2ECS), 2023, pp. 732–735.
- [18] A. Raj, C. Sarkar, and M. Pathak, "Thermal and multiphase flow simulations of polytetrafluoroethylene-based grease flow in restricted geometry," *Proc. Inst. Mech. Eng. J: Eng. Tribol.*, 2022, vol. 236, no. 1, pp. 80–89.
- [19] D. Fischer, S. von Goeldel, G. Jacobs, and A. Stratmann, "Numerical investigation of effects on replenishment in rolling point contacts using CFD simulations," *Tribol. Int.*, 2021, vol. 157, p. 106858.
- [20] J. Wang, M. P. Pandya, and F. Greco, "Detection of active grease reservoirs in bearings by CFD," *Tribol. Int.*, 2023, vol. 179, p. 108146.
- [21] S. Zhang, G. Jacobs, S. Vafaei, S. von Goeldel, and F. König, "CFD investigation of starvation behaviors in a grease lubricated EHL rolling contact," *Forsch. Im Ingenieurwesen*, 2023, vol. 87, no. 1, pp. 353–362.
- [22] S. Zhang, G. Jacobs, S. von Goeldel, S. Vafaei, and F. König, "Prediction of film thickness in starved EHL point contacts using two-phase flow CFD model," *Tribol. Int.*, 2023, vol. 178, p. 108103.
- [23] S. Zhang, B. Klinghart, G. Jacobs, S. von Goeldel, and F. König, "Prediction of bleeding behavior and film thickness evolution in grease lubricated rolling contacts," *Tribol. Int.*, 2024, vol. 193, p. 109369.
- [24] E. O. Forster and J. J. Kolfenbach, "Viscoelastic behavior of greases," ASLE Trans., pp. 13-24, 1958.
- [25] G. M. Gow, "The CEY to grease rheology," *Trans. Mech. Eng.*, The Institution of Engineers, Australia, Special Issue Tribology, vol. ME16, no. 3, pp. 202–205, 1991.
- [26] I. Couronné, G. Blettner, and P. Vergne, "Rheological behavior of greases: Part I—Effects of composition and structure," *Tribol. Trans.*, vol. 43, no. 4, pp. 619–626, 2000.
- [27] A. W. Sisko, "The flow of lubricating greases," *Ind. Eng. Chem.*, 1958, vol. 50, pp. 1789–1792.
- [28] K. D. Bogie and J. Harris, "The rheology of greases," Rheol. Acta, 1968, vol. 7, pp. 255.
- [29] H. E. Mahncke and W. Tabor, "A simple demonstration of flow type greases," Lubr. Eng., 1955, vol. 11, pp. 22.
- [30] C. R. Singleterry and E. E. Stane, "Rheological properties of lubricating greases," Colloid. Sci., 1951, vol. 6, pp. 171.
- [31] W. Herschel and R. Bulkley, "Measurement of consistency as applied to rubber-benzene solutions," *Am. Soc. Test. Mater.*, *Proc.*, 1926, vol. 26, pp. 621–633.
- [32] M. N. Mastrone and F. Concli, "CFD simulation of grease lubrication: Analysis of the power losses and lubricant flows inside a back-to-back test rig gearbox," *J. Non-Newtonian Fluid Mech.*, 2021, vol. 297, p. 104652.
- [33] DIN 51810-1.